Spin-catalyzed hopping conductivity in disordered strongly interacting quantum wires

S. A. Parameswaran[1,2] and S. Gopalakrishnan[2,3,4]

[1]*Department of Physics and Astronomy, University of California, Irvine, California 92697, USA*
[2]*Kavli Institute for Theoretical Physics, University of California, Santa Barbara, California 93106, USA*
[3]*Department of Physics and Burke Institute, California Institute of Technology, Pasadena, California 91125, USA*
[4]*Department of Engineering Science and Physics, CUNY College of Staten Island, Staten Island, New York 10314, USA*

(Received 29 June 2016; revised manuscript received 27 October 2016; published 6 January 2017)

In one-dimensional electronic systems with strong repulsive interactions, charge excitations propagate much faster than spin excitations. Such systems therefore have an intermediate temperature range [termed the "spin-incoherent Luttinger liquid" (SILL) regime] where charge excitations are "cold" (i.e., have low entropy) whereas spin excitations are "hot." We explore the effects of charge-sector disorder in the SILL regime in the absence of external sources of equilibration. We argue that the disorder localizes all charge-sector excitations; however, spin excitations are protected against full localization, and act as a heat bath facilitating charge and energy transport on asymptotically long time scales. The charge, spin, and energy conductivities are widely separated from one another. The dominant carriers of energy in much of the SILL regime are neither charge nor spin excitations, but neutral "phonon" modes, which undergo an unconventional form of hopping transport that we discuss. We comment on the applicability of these ideas to experiments and numerical simulations.

DOI: 10.1103/PhysRevB.95.024201

I. INTRODUCTION

In models of electrons with strong repulsive interactions—such as the large-U Hubbard model, the t-J model or the Wigner crystal—the characteristic energies of charge and spin excitations are widely separated. For instance, in the Hubbard model at large interactions U, charge excitations have an energy scale set by the hopping t, whereas spin excitation energies are set by the exchange scale $J = t^2/U \ll t$. When the temperature of the system lies between these two widely separated scales, the charge degrees of freedom are "cold" (i.e., essentially in their ground state) whereas the spins are "hot" (i.e., close to infinite temperature [1–4]). In one dimension, this intermediate-temperature regime is called a "spin-incoherent Luttinger liquid" (SILL) [5]. In the SILL, charge degrees of freedom are at low temperature and thus form a Luttinger liquid [6], whereas the spin degrees of freedom are at infinite temperature and are therefore trivial from the point of view of thermodynamics and static correlations. The SILL is thus a tractable regime of these strongly interacting models that is conceptually (and phenomenologically [5]) quite distinct from the conventional Luttinger-liquid regime [7], where both charge and spin excitations are "cold."

Because spin excitations in the SILL regime are effectively at infinite temperature, their equilibrium density matrix is close to the identity, so the *thermodynamic* properties of the SILL are independent of the spin energy scale. Although degrees of freedom at infinite temperature do not contribute to *thermodynamics*, they can still govern *dynamics*. This situation obtains, for example, in disordered *isolated* quantum systems, which undergo a many-body localization (MBL) transition [8,9] even at infinite temperature [10] (see Refs. [11,12] for recent reviews). We argue here that a similar situation arises in the disordered, isolated SILL. The charge excitations alone would be localized by disorder, causing the intrinsic charge relaxation time scale to diverge. Instead, the dominant mechanism for charge dynamics involves transitions that borrow energy from the "hot" spin bath—the spins "catalyze" conduction by placing processes on shell that in their absence would be forbidden due to energy conservation. The SILL regime is an unusual setting for exploring such phenomena: prior studies of MBL have involved systems *all* of whose degrees of freedom are cold [8] or hot [10], whereas in the SILL some degrees of freedom are cold and others are hot.

Understanding transport and relaxation in this regime is important, first, because experimental proposals for realizing the SILL regime tend to involve systems that are well-isolated from their environments and temperatures where phonon-mediated relaxation is unimportant. Moreover, relaxation in "two-component" systems—involving high-frequency, tightly localized modes coupled to low-frequency delocalized modes—naturally arises in multiple experimental settings. For instance, the experiments of Ref. [13] involve quasi-1D geometries, in which localized longitudinal modes can relax by coupling to delocalized transverse modes whose bandwidth is tunable by varying lattice depth; in solid-state systems, nuclear spins can play a similar role in thermalizing the dynamics of electron spins. While such "narrow-bath" systems ultimately establish ergodic dynamics, the crossover to such behavior occurs over asymptotically long time scales: the dynamics at shorter times may retain imprints of the (avoided) localized phase, e.g., via the parameter dependence of relaxation time scales [14]. As true many-body localization is an experimentally elusive ideal—particularly in the solid-state setting—understanding such dynamical crossovers is an important route to study various intriguing phenomena that have been proposed to occur in the MBL regime and proximate to the localization transition [15–19].

Accordingly, here we advocate that the disordered SILL is profitably viewed as an instance of a "nearly many-body localized metal" [14], and consequently studying its transport properties may provide insight into universal properties of many-body localized systems in one dimension. Specifically, we argue that transport in isolated disordered wires in the SILL regime is governed by the small spin energy scale,

 ©2017 American Physical Society

since in the absence of the thermalizing spin bath, the system is (many-body) localized. We consider a hierarchy of scales in which the charge energy scale is the largest in the problem, followed successively by the disorder strength, the temperature, and the spin energy scale. In this regime, disorder localizes the low-energy charge excitations.[1] Thus charge excitations on their own do not give rise to transport in the dc limit. However, the spin excitations act as a slowly fluctuating thermal bath (which is protected from localization by the SU(2) spin-rotation symmetry, provided that spin-orbit coupling is absent). Charge and energy transport then take place through various forms of variable-range hopping mediated by this slowly fluctuating internal spin bath. The resulting energy transport is parametrically faster than charge transport, but both rates show a nontrivial power-law dependence on the spin energy scale. We discuss how this spin-catalyzed hopping conductivity can be tested in both cold-atom and solid-state experiments as well as in numerical simulations.

Before proceeding, we place the present paper in the context of other related work. Previous investigations of transport in SILLs [20] have focused on single-impurity problems, rather than the case of a finite density of quenched impurities that is pertinent to localization physics. Hopping conductivity (both dc and ac) in Luttinger liquids has been recast in terms of effective two-level systems [21,22] and pinned charge-density waves [23–27], but those prior works all assumed the existence of a "perfect bath" capable of placing any hopping process on-shell; this is in marked contrast to the narrow-bandwidth bath, natural in the SILL context, that we consider here. In addition, the SILL is *not* a conventional Luttinger liquid regime: although an effective Luttinger liquid description exists for the charge sector, the spin sector is at very high temperatures and cannot be described as a Luttinger liquid. The phenomenology of "narrow bath" disordered systems was studied in Ref. [14] but there the focus was on developing a mean-field approach to the MBL transition, rather than on transport properties. Furthermore, in contrast to many analytical treatments of MBL that work in the limit of a weakly interacting Anderson (i.e., free-fermion) insulator, the approach here builds in strong interactions at the outset. We focus on the case of relatively weak disorder; other effects can emerge at strong disorder [28,29]. Finally, we note that while variable-range hopping conductivity is a well-known low-temperature transport phenomenon in disordered semiconductors, the mechanism we discuss for the thermal conductivity κ of the SILL (Sec. VI) has no obvious parallels in other systems. We argue that κ is dominated by the spin-mediated hopping of neutral phononlike bosonic excitations. The number of these neutral bosons is not explicitly conserved; however, because their energy scale is much greater than the spin energy scale, the neutral bosons cannot decay into spin excitations except at very high orders in perturbation theory. Thus their number is approximately conserved, and they contribute to κ through incoherent hopping.

[1]In principle, high-energy charge excitations that lie outside our effective theory can provide activated transport; at the temperatures of interest, however, this mechanism is subleading to what we consider.

The rest of this paper is structured as follows. In Sec. II, we provide a heuristic discussion of the SILL within the "fluctuating Wigner solid model" that allows us to review standard results on the SILL regime and introduce some key features relevant to the addition of quenched disorder in this regime. In Sec. III, we provide a more "universal" Hamiltonian that captures key features of the disordered SILL and comment on the energy scales and excitations relevant to our discussion. We then discuss the special features of these excitations in the *isolated* SILL at finite energy density in Sec. IV. In Sec. V, we discuss both ac and dc charge conductivity. In Sec. VI, we estimate the dc thermal conductivity, which we argue is parametrically larger than the dc charge conductivity. Finally, in Sec. VII, we summarize our results and discuss the effects of phonons and spin-orbit coupling, as well as implications for experiment.

II. HEURISTIC DISCUSSION OF THE DISORDERED SILL

In this section, we motivate our discussion of the phenomenology of the SILL regime, for concreteness considering a specific microscopic model: the fluctuating Wigner solid [5] of spin-1/2 electrons. Many of the key features of the clean, and the disordered, SILL regime are manifest in this model, and can be explored in a tractable semiclassical limit. We emphasize that the SILL regime is generic in strongly interacting one-dimensional systems; we shall turn to this general situation in subsequent sections.

A. Fluctuating Wigner-solid model

The fluctuating Wigner-solid or harmonic-crystal model [5] has the microscopic Hamiltonian

$$H_{\mathrm{WS}} = \sum_{i=1}^{N} \frac{p_i^2}{2M} + \frac{M\omega_0^2}{2}(x_i - x_{i+1} - 1)^2, \tag{1}$$

where M is a particle mass, and (x_i, p_i) are position and momentum coordinates of the ith particle. In two or more dimensions, this model has a crystalline phase at zero temperature; in one dimension, however, long-range crystalline order is absent even at zero temperature for finite M. (In the $M \to \infty$ limit, of course, the ground state is a classical charge density wave.) Nevertheless, in the limit of large M, the typical root-mean-squared displacement of a particle (in the background potential created by the other particles) is much less than the interparticle spacing. Thus, if the particles comprising the Wigner solid are spin-1/2 fermions, their exchange effects (and thus the spin energy scale) are strongly suppressed. The ratio of spin bandwidth W_s to charge bandwidth W_c vanishes, at large M [30], as $W_s/W_c \sim \exp(-\text{const.} \times \sqrt{r_s})$, where r_s is the interparticle spacing. At temperatures in the intermediate regime $W_s \ll T \ll W_c$, the spin degrees of freedom are effectively at infinite temperature, but the charge degrees of freedom can be regarded as a *spinless* Luttinger liquid [5] with an effective Luttinger parameter K_{eff} that goes to zero algebraically with $1/M$ [31]. This is the SILL regime of the fluctuating Wigner solid.

B. Effects of disorder in the classical limit

The disorder we consider consists of a random potential, of width D and correlation length much smaller than the interparticle spacing, acting on the total fermion density, i.e.,

$$H_{\text{dis.}} = D\sum_{i=1}^{N} V(x_i),$$
$$\langle V(x)V(x')\rangle \sim e^{-\Lambda|x-x'|}, \tag{2}$$

where Λ is short compared with the other length scales in the problem. The disorder couples directly only to the charge degrees of freedom. Let us first consider the $M \to \infty$ classical limit. In this limit, the Imry-Ma argument [32] suggests that long-range crystalline order is unstable for arbitrarily weak disorder; instead, disorder locally "pins" the charge-density wave [23,25,26], and the pinning scale is given [25,26] by $\xi_p \sim 1/D^{1/3}$. On scales shorter than this, the system looks crystalline; however, spatial correlations on length scales large compared with ξ_p are exponentially decaying.

C. Effects of disorder for large finite M

We now perturb away from the above classical limit, which can be regarded as the $K_{\text{eff}} \to 0$ limit of a Luttinger liquid. For $K_{\text{eff}} \to 0$, charges are arranged in their lowest-energy classical configuration [25]. Low-energy quantum fluctuations about this configuration for small but nonzero K are of two kinds: (i) oscillations of a particle about its classical position (the "Gaussian" or "phonon" sector) and (ii) tunneling events between nearly degenerate classical configurations (the "instanton" sector [24]).

Low-energy excitations in both sectors are localized, but as we now argue they have different characteristic localization lengths [33]. It is helpful to think of the system as consisting of randomly coupled segments of clean CDW, each of size $\sim\xi_p$. Gaussian-sector excitations (which involve oscillations with characteristic single-particle displacements l_{osc} much smaller than the interparticle spacing) are correlated over distances $\sim\xi_p$; this is their characteristic localization length. (As these are phonons of the CDW and disorder explicitly breaks translational symmetry, they are not protected against localization at any energy—and hence the conclusions of [34] do not apply here.) Instanton-sector excitations, by contrast, involve charge motion over distances that are large compared with a lattice spacing (and, in the regimes we shall focus on, large compared with ξ_p as well). Consider an instanton that moves charge between two nearly degenerate positions separated by a distance L. This process involves tunneling through a barrier with a width $\sim L$ and a height that depends on the interaction strength, and its matrix element is thus suppressed exponentially in L, with a coefficient that vanishes in the classical limit. We define a "quantum length" ξ_q through the condition that the instanton matrix element falls off as $\exp(-L/\xi_q)$. In general, $\xi_q \ll \xi_p$ whenever $K_{\text{eff}} \ll 1$.[2] Figure 1 sketches the two types of charge sector excitations.

[2]The existence of multiple relevant length scales is pointed out in Ref. [33], and relations between the various length scales are derived there. The length scale we term ξ_q is related to the scale labeled $\xi_{\text{tun.}}$ in that work. For our purposes, it will suffice to treat these various relevant length scales as separate parameters.

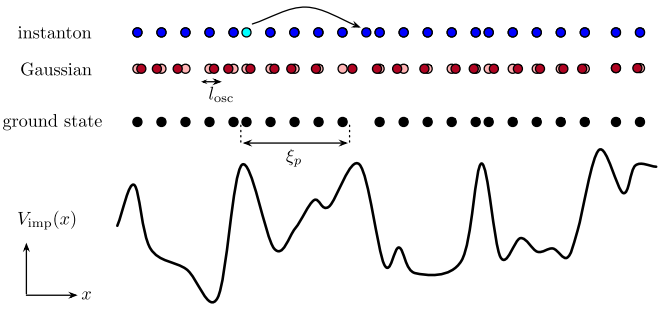

FIG. 1. Gaussian modes vs instantons. In the presence of an impurity potential $V_{\text{imp}}(x)$, near the classical ($K \to 0$) limit the ground-state configuration of the SILL is a pinned CDW (black dots), retaining short-range density-wave order on scales of order the pinning length ξ_p. Excitations of this pinned CDW, may be divided into (i) Gaussian (quantum or thermal) fluctuations of the charges about their equilibrium configuration (red dots) with amplitudes l_{osc} much smaller than the inter-particle spacing, and (ii) instanton events (blue dots) that describe quantum tunneling between nearly degenerate classical saddle points. The instantons involve large-scale charge rearrangements, whereas the Gaussian modes can transmit energy, but not charge, over long distances. All hopping processes of relevance to transport occur on asymptotically longer scales, as discussed in the main text.

D. Induced exchange dynamics

The kinetic energy term at finite M not only induces dynamics in the charge sector (viz. the excitations discussed above), but also gives rise to exchange processes and thus *spin* dynamics. By symmetry, the effective interaction between two spins is of the Heisenberg form. In the semiclassical limit, the magnitude of this effective interaction falls off as $W_s \sim W_c \exp(-\text{const.} \times \sqrt{r_s})$ where r_s is the typical interparticle spacing [30]. The randomness in equilibrium charge positions implies that the spin Hamiltonian is of the random-bond Heisenberg form. Such random-bond Heisenberg models are believed not to exhibit localization at high temperatures [35]. Moreover, for weak pinning ($\xi_p \gg 1$, in units of the lattice spacing), the exchange randomness is slowly varying (on a scale ξ_p). The appropriate description for interacting spins at high temperature in the presence of smoothly varying randomness is *hydrodynamic* [36]: the spins achieve local thermal equilibrium on a time scale of order $1/W_s$ and on longer time scales their dynamics is diffusive, with a diffusion constant set by $D_s \sim 1/W_s$.

Thus, on timesales $\sim 1/W_s$, the spins equilibrate in a fixed charge background. On time scales that are long compared with $1/W_s$, the spins act as a bath allowing for charge dynamics. Because the spin bath is slowly fluctuating [14], it can only act as a bath for charge rearrangements that change the energy of the charge sector by $\lesssim W_s$. Such transitions, as we shall see in the following sections, are typically sufficiently collective that the associated matrix elements are much smaller than W_s. This justifies treating spin-mediated charge transitions using the Golden rule, as noted, e.g., in Ref. [37].

III. UNIVERSAL MODEL OF THE DISORDERED SILL

The discussion in the previous section focused on the case of the fluctuating Wigner solid; however, the SILL regime

exists more generally in strongly interacting one-dimensional systems [5]. Therefore, before turning to a more quantitative discussion of transport in the disordered SILL, we specify a general, "universal" Hamiltonian that captures the key general features of the disordered SILL regime. This general Hamiltonian consists of three parts, $H = H_c + H_s + H_{sc}$, respectively, denoting terms that act exclusively on the charge sector, terms that act exclusively on the spin sector, and terms that couple the two sectors. The charge sector Hamiltonian is of the Luttinger liquid form,

$$H_c = \frac{v_{\rm eff}}{2\pi}\int dx\left\{K_{\rm eff}[\partial_x\theta(x)]^2 + \frac{1}{K_{\rm eff}}[\partial_x\phi(x)]^2\right\} + \int dx\, D(x)e^{i\phi(x)+ik_F x} + \text{H.c.}, \tag{3}$$

where ϕ,θ are collective variables that parametrize density and phase fluctuations [7], and the velocity $v_{\rm eff}$ and Luttinger parameter $K_{\rm eff}$ are what they would be for a spinless system at the relevant density [5]. Note that $K_{\rm eff} = 2K_c$, where K_c is the charge Luttinger parameter of the conventional zero-temperature Luttinger-liquid phase of the model (which sets in at temperatures much lower than the spin exchange scale, and with which we shall not be concerned in this work). The second line of (3) represents the backscattering terms due to the disorder potential [23,28]; these produce an impurity scattering rate $\sim D^2$, which is the characteristic disorder scale that we compare with W_s. Associated with this charge Hamiltonian are two characteristic localization lengths, ξ_p and $\xi_q \lesssim \xi_p$, as discussed in the previous section. An important point is that the ratio ξ_q/ξ_p, while small in the Wigner-crystal case, is not always small for other models that have a SILL regime; for instance, in the Hubbard and t-J models, the two lengths are of the same order of magnitude. (Note that we have written (3) in variables appropriate to the SILL regime, so ϕ,k_F represent parameters of the effective spinless fermions. In order to transform back to variables ϕ_c,k_F^c appropriate to the (spinful) electrons we may use the relations $\phi_c = \sqrt{2}\phi$ and $k_F = 2k_F^c$ [20].)

The spin Hamiltonian H_s is taken to have some generic local lattice form, in terms of local operators h_i:

$$H_s \simeq W_s \sum_i \hat{h}_i, \tag{4}$$

where the $\hat{h}_i$ are chosen so that H_s is invariant under SU(2) rotations. In the SILL regime, the overall energy scale W_s is small enough that $\exp(-H_s/T) \approx 1$. Thus the spin Hamiltonian does not affect thermodynamics or equilibrium properties in this regime—a feature known as "superuniversality" [5]. Since we are interested in *dynamics* as well as thermodynamics, we specify that the long-time autocorrelation functions of the spin Hamiltonian follow linearized hydrodynamics. Thus, for example,

$$\left\langle S_i^x(t)S_i^x(0)\right\rangle \sim 1/\sqrt{\mathcal{D}t}, \tag{5}$$

where $\mathcal{D} \sim W_s$ is the spin diffusion constant. Additionally, nonconserved operators will decay exponentially with a rate that is similarly set by W_s. These assumptions would hold, in particular, if the high-temperature dynamics of H_s were thermal and ergodic, as they generically will be, absent many-body localization—a possibility excluded in this work by assuming SU(2) spin-rotation symmetry throughout.

The spin-charge coupling is given by a generic SU(2)-symmetric form, such as

$$H_{\rm sc} \simeq g\sum_i \int dx\, \hat{h}_i[\partial_x\phi_c(x)]^2\delta(x - x_i), \tag{6}$$

where x_i is the position of the ith lattice site. The origin of the spin-charge coupling is, as discussed above, that the spin exchange scale is sensitive to the charge positions. We emphasize that there is no general reason that the spin-charge coupling constant g should be small compared with the spin energy scale W_s. In this respect, the SILL is distinct from the conventional Luttinger liquid: the conventional Luttinger liquid is a renormalization-group fixed point at which charge and spin decouple [7], because all spin-charge couplings are irrelevant in the renormalization group sense. By contrast, the SILL regime is not a *fixed point* so this argument does not apply to it. As a corollary, it also follows that higher-order spin-charge couplings may also be present with significant strength. Our conclusions are unchanged as long as (1) these do not break SU(2) symmetry and thereby provide a route for the spins to localizes due to 'feedback' from the charge; and (2) the spin degrees of freedom always have a very narrow bandwidth, that limits their capacity to thermalize the charges despite the potentially large terms coupling the two sectors (as illustrated in Sec. II D above). In this regime, despite the strong coupling, it is permissible to treat the effect of the spin bath using Fermi's golden rule. A detailed analysis of the validity of this approximation is given in Ref. [14].

IV. ISOLATED DISORDERED SILL AT FINITE ENERGY DENSITY

In previous sections, we introduced the two kinds of low-energy excitations of the pinned CDW: approximately Gaussian phonons with a localization length ξ_p and instantons (which are nonlocal two level systems that one can regard as fermions) that have a localization length ξ_q. We now consider how the properties of these different excitations are affected at low but finite energy density.

A. Gaussian sector

The Gaussian sector consists of bosonic modes at frequency ω_p, generically with anharmonicities; at finite temperature these modes will be thermally occupied. One can partition these bosonic modes into "classical" modes (for which $T \gg \omega_p$, with occupation[3] $\sim T/\omega_p$), and "quantum" modes, which are close to their ground state, and have occupancy $\sim \exp(-\omega_p/T)$. The density of states goes as ω_p^3 at low frequencies [38]; we assume that the temperature is such that all relevant modes are in this low-frequency tail.

[3]This is likely an overestimate because anharmonicities will tend to limit mode occupancy. We will see later that, even overestimating their occupation, these modes do not dominate response.

B. Instanton sector

Instantons with a splitting much smaller than T are essentially at infinite temperature, whereas those with splitting much larger than T are in their ground state. Our interest is mainly in the low-frequency limit $\omega_i \ll T$, so the instantons with splitting $\omega_i \gtrsim T$ will be mostly irrelevant to our analysis.

When interaction effects are absent, therefore, the relevant degrees of freedom are a thermally occupied ensemble of localized bosonic modes (with localization length ξ_p) and localized fermionic modes (with localization length $\xi_q \ll \xi_p$). Adding interactions at finite temperature alters this picture in three ways. First, interactions couple the localized low-energy excitations of the CDW to high-energy charge modes (with energies $\sim W_c$), which are presumably delocalized in the weakly disordered, strongly interacting limit of interest to us (but see Refs. [39,40]). These delocalized modes can transport charge and act as a bath for the low-energy sector. However, their effects are suppressed by the Boltzmann factor $\exp(-W_c/T)$, and will be subleading in the $W_c \ll T$ regime of interest to us. Second, interactions permit many-body resonances, involving the simultaneous rearrangement of several particles [41–44]; such processes (that we describe in more detail below) are absent in the ground state (which is unique) but possible in thermal states (which have a finite entropy), and will be relevant to our discussion of transport below. This feature is absent in the ground-state, finite-frequency case studied in Ref. [38], and is responsible for the qualitative difference between our results and those of Ref. [38]. Third, it is in principle possible for very low-frequency "classical" modes from the Gaussian sector to delocalize the system, because they may act as local low-frequency drives. Before proceeding, we must ensure that this situation does not arise in the SILL in the dynamical regimes of interest to us.

C. Stability against Gaussian-sector driving

That these spatially sparse classical modes do not delocalize the rest of the system can be seen by the following heuristic argument. The criterion for a drive at strength A and frequency ω to cause delocalization [45] is that

$$\left(\frac{A}{\omega}\right)\left(\frac{A}{W_c}\right)^{2/(\xi_p \ln 2)} \gtrsim 1. \tag{7}$$

Because the classical modes are themselves localized, at a distance x from such a classical mode, the amplitude of its coupling to other modes (and thus the effective drive amplitude) is $A \sim W_c \exp(-x/\xi_p)\sqrt{T/\omega}$ (the factor of $\sqrt{T/\omega}$ is due to Bose enhancement). The spacing between classical modes of frequency ω is set by $x(\omega) \sim (W_c/\omega)^3$, using the estimate for the tail density of states. In order for the rare localized modes at frequency ω to delocalize the entire system, the criterion (7) would have to be satisfied at distances of order $x(\omega)$, so that each mode can localize the region around it. This would require that

$$\frac{W_c}{T}\left(\frac{T}{\omega}\right)^{\frac{3}{2}+\frac{1}{\xi_p \ln 2}} \exp\left[-\left(\frac{W_c}{\omega}\right)^3\left(\frac{1}{\xi_p}+\frac{2}{\xi_p^2 \ln 2}\right)\right] \gtrsim 1, \tag{8}$$

which is clearly not the case for sufficiently small ω. Thus, rare classical modes might cause some degree of delocalization in their immediate surroundings, but do not delocalize the entire system. [We emphasize that (8), which does not consider anharmonicity and treats the modes as purely classical, *overestimates* the extent of delocalization due to these modes.]

D. Delocalization via spin bath

So far, we have ignored the spin degree of freedom completely, and have found that under this assumption the system is effectively localized at finite temperature (up to time scales of order $\exp(-W_c/T)$). As discussed in Secs. II D and III, the effective coupling between spin and charge is weak enough to permit treating the spin bath at the Golden rule level (but keeping in mind that it is narrow bandwidth). We emphasize, however, that because of the SU(2) symmetry of the spin sector, spin excitations do not freeze out at high temperature, and some transport is present even in the limit of $g \gg W_s$. (Note that this conclusion will be altered if SU(2) symmetry is broken, e.g., by spin-orbit coupling: in this case, the localized charge distribution can induce a site-dependent random field on the spin sector, and such back-action may localize the bath—a so-called "MBL proximity effect" [46]. In the SU(2) symmetric case, only bond disorder is induced on the spins, and this is believed to be robust against MBL [35].)

Owing to the scale hierarchy $W_s \ll T$, the manner in which the spin bath delocalizes the charge sector is an unusual form of variable-range hopping. Because the spin sector can only absorb energies smaller than W_s, the transitions that it mediates involve pairs of states that are within W_s of one another in energy. The effects of such coupling on relaxation in the instanton sector were previously addressed in Ref. [14]; below, we generalize these results to transport. The effects of $W_s \ll T$ on the *Gaussian* sector, however, are more unusual. Here, the combination of localization and the narrow spin bath gives rise to an approximate boson number conservation: although bosons can be created or destroyed, it takes an energy $\sim T$ to create and destroy them, so the relevant process only takes place at order $T/W_s \gg 1$ in the spin-charge coupling. The dominant channel by which phonons equilibrate, instead, is by hopping between approximately degenerate modes. This is related to a peculiar feature of the spin "bath"; namely, that its heat capacity is far lower than that of the charge sector. As a consequence, the relaxation of a nonequilibrium charge configuration does not appreciably change the energy of the spin sector: rather, the spin sector primarily "catalyzes" the spreading of energy within the charge sector, by permitting charge transitions that would not otherwise be on shell.

We have now set the stage for our main discussion: in the next two sections, we will consider charge and energy transport through hopping processes of the Gaussian and/or instanton sectors of the charge modes, that are placed on-shell by rearrangements of the thermalizing spin bath.

V. CHARGE TRANSPORT

In this section, we discuss charge transport in the disordered SILL. We begin by discussing the isolated-system result for linear-response charge conductivity due to the instanton sector. We then turn to saturation effects induced by the spin bath, and then finally to conductivity in the dc limit. Our discussion of

ac response—which does not involve the spin bath—is similar in spirit to previous work [22,41]; however, in the dc limit the narrow-band nature of the spin bath leads to striking deviations from the standard hopping-transport predictions [47,48].

A. Optical conductivity in the isolated system

We begin by considering the optical charge conductivity (ignoring the spin degree of freedom). For this purpose, it is convenient to begin with the Kubo formula,

$$\sigma(\omega) = \frac{1 - e^{-\omega/T}}{\omega Z N} \sum_{m,n} e^{-E_m/T} |\langle m|j|n\rangle|^2 \delta(\omega - \omega_{mn}),$$

where Z is the partition function, N the number of sites in the system, the indices m,n run over all the many-particle eigenstates, whose splitting is given by ω_{mn}, and the current j is the sum over local currents, $j = \sum_i j_i$.

We are interested in the frequency regime $W_s \ll \omega \ll T \ll W_c$. Thus we can approximate $1 - e^{-\omega/T} \approx \omega/T$. The Boltzmann factors $e^{-E_m/T}/Z$ determine a density per site $\sim T/W_c$ of relevant initial states. In this regime, and in the absence of interactions, the dominant contribution to the optical conductivity comes from two-level systems (TLSs) consisting of two-site resonances with a splitting that matches the drive at frequency ω. The optical conductivity due to these was derived by Mott [49], whose argument we briefly review for completeness. The characteristic size of resonant pairs with splitting ω is r_ω, determined by the condition $W_c e^{-r_\omega/\xi_q} \sim \omega$; the current matrix element of the drive coupling these pairs is $j \sim \omega r_\omega$ [49]. Finally, the phase space of final states goes as $r_\omega^{d-1}\xi_q/W_c$ in d dimensions (and is therefore constant in one dimension). Combining these expressions, we recover the standard expression

$$\sigma_{\rm sp}(\omega) \sim \left(\frac{\omega}{W_c}\right)^2 \xi_q^3 \ln^2\left(\frac{W_c}{\omega}\right). \tag{9}$$

At finite temperature, in the presence of interactions, this expression is modified because multiparticle rearrangements become possible [41]. The low-temperature Hamiltonian of the spinless CDW can be written schematically in terms of instanton configurations τ_α (which are two-level systems) as $H = \sum_\alpha h_\alpha \tau_\alpha^z + \sum V_{\alpha\beta}\tau_\alpha^i \tau_\beta^j + \ldots$; here, i,j run through the Pauli indices x,y,z and α,β denote the location of the instanton. Higher-order interactions fall off with the order of the interaction and also fall off exponentially with the distance between the instantons involved, with a characteristic localization length ξ_p. (It might naively seem that the falloff should be governed by the instanton size $\sim\xi_q$. However, instantons can experience interactions that are mediated by the Gaussian sector, which is less tightly localized.) At low temperatures, thermally occupied instantons are sparse, so we can use perturbation theory in the instanton-instanton interaction $V_{\alpha\beta}$ to argue that n-particle rearrangements have a matrix element that falls off exponentially with n.

Following Ref. [41], we can then generalize Mott's argument as follows. Given a drive frequency ω, we seek n-particle rearrangements with a rate $\sim\omega$. The phase space is much greater than in Mott's estimate: specifically, the number of possible n-particle rearrangements involving a particular particle goes as e^{sn} where $s \simeq T/W_c$ is an entropy density per site (one can also think of s as the density of excited sites). Since the excitation density is low ($\sim s$), the interactions between excitations are also weak in the low-temperature limit: the tunneling matrix element for a two-particle rearrangement will fall off as the wave function overlap between the two localized orbitals at a distance $1/s$, which is $\exp(-1/(s\xi_p))$. Thus an n-particle rearrangement has tunneling matrix element $W_c \exp(-n/(s\xi_p))$ (replacing the single-particle result $W_c e^{-r/\xi_q}$). This highlights an important but subtle aspect of the many-body Mott argument; namely, the size of the matrix elements involved in the Mott resonant transitions (and thus the size of optimal rearrangements) is set solely by the external frequency; the amount of conductivity due to these thus depends mostly on the phase space of available rearrangements with a particular matrix element. Therefore, even though the matrix element between initial and final many-body states is smaller for a multiparticle rearrangement this is compensated by the much larger phase space for such processes and thus these rearrangements dominate the conductivity.

Using the Mott criterion, the optimal rearrangements at frequency ω involve $n_\omega \simeq s\xi_p \ln(W_c/\omega)$. The *current* matrix elements that enter the Kubo formula retain their dependence on ω (up to logarithmic factors), so that, upon including the many-body phase space factor for the optimal rearrangements, we find

$$\sigma_{\rm int}(\omega) \sim \left(\frac{\omega}{W_c}\right)^{2-\gamma\xi_p(T/W_c)}, \tag{10}$$

where γ is a numerical factor of order unity. Note that these interaction effects are only relevant at sufficiently low frequencies, $\omega \lesssim W_c e^{-W_c/(T\xi_p)}$. At higher frequencies, the many-body resonances giving rise to Mott-type conductivity are absent, and the single-particle result (9) applies.

Coupling to the spin bath does not appreciably change this linear-response result in the regime $W_s \ll \omega \ll T$. However, it does affect the nature of the *steady-state* response [22]. When dissipation is absent, linear response only occurs as a transient, on time scales short compared with the field amplitude $t \lesssim 1/(\xi_q E)$. On longer time scales, all the instantons are saturated and there is no further response [50–52]. However, in the presence of a relaxation time scale τ (which we will estimate below), the steady-state conductivity is given by [22]

$$\sigma_{\rm ss}(\omega) \simeq \sigma_{\rm int}(\omega)\left[1 - \left(\frac{E\xi_q \ln(W_c/\omega)}{1/\tau}\right)^2\right]. \tag{11}$$

B. Relaxation in the presence of the spin bath

Before turning to the dc conductivity (which is governed by hopping processes mediated by the spin bath), we briefly discuss the rate at which a particular local configuration of charge is excited or de-excited by means of the spin bath. (This is a straightforward application of the ideas in Ref. [14].) Because the spin bath has bandwidth $\sim W_s$, only transitions that change the energy of the charge sector by $\lesssim W_s$ are permitted. This rules out most local charge rearrangements, which change the energy by $\sim W_c$. The lowest-order processes with energy denominator $\lesssim W_s$ are therefore (i) single-charge tunneling: assuming a constant density of states ρ_0, the range over which a

single charge can hop while remaining on-shell is estimated by demanding that we find within an energy window of order W_s over scale l: in other words, we require that $\rho_0 W_s l^d \sim 1$. Using $d = 1$ and $\rho_0 \sim 1/W_c$, we find that this process must occur over a distance $l \sim W_c/W_s$. The matrix element for single-charge tunneling is therefore $g e^{-l/\xi_q} \sim g \exp[-W_c/(\xi_q W_s)]$ where g is the spin-charge coupling. Recalling that the density of final states is set by the spin bath and is therefore $\sim 1/W_s$ and applying the Golden rule, we find an associated rate

$$\Gamma_{\rm sp} \simeq \frac{g^2}{W_s} e^{-2W_c/(\xi_q W_s)}. \tag{12}$$

Note that this is temperature-independent, so one might expect it to dominate in some temperature regimes over the temperature-dependent processes.

(ii) Multiparticle rearrangements: with interactions, we may simultaneously rearrange an appreciable fraction of particles in some region while remaining on shell. The estimate for this closely parallels the many-body Mott conductivity discussion above: we consider a region of size l, so that the multiparticle charge rearrangements of this region accessible with an entropy density per site $s \sim T/W_c$ have an effective energy level spacing $\delta(l) \sim W_c e^{-sl}$. Requiring that such processes can be placed on shell by the spin bath [i.e., setting $\delta(l) \sim W_s$] yields $l \sim 1/s \ln W_c/W_s$. The matrix element for such a transition is $g \exp(-l/\xi_p)$, where g is again the spin-charge coupling (ξ_p enters, rather than ξ_q as it is the relevant scale for multiparticle rearrangements); again applying the Golden rule with final density of states $\sim 1/W_s$, we find

$$\Gamma_{\rm int} \simeq \frac{g^2}{W_s} \left(\frac{W_s}{W_c}\right)^{2W_c/(\xi_p T)}. \tag{13}$$

Note that the temperature-dependence is *activated*.

Comparing Eqs. (12) and (13), one finds that interacting processes dominate when

$$T \gtrsim W_s \ln(W_c/W_s), \tag{14}$$

while single-particle hops dominate relaxation (and the relaxation rate thereby becomes temperature-independent) in the window $W_s \ll T \ll W_s \ln(W_c/W_s)$.

C. Hopping conductivity

It is straightforward to extend the previous analysis from relaxation to hopping transport. Because $W_s \ll T$, any pair of states or configurations within W_s in energy automatically have an energy separation much less than T. It is therefore unnecessary to optimize over activation barriers (as in the standard variable-range hopping analysis [47]). Rather, the range over which hopping takes place is determined by the spacing between sites (or configurations) that are within W_s in energy; the associated rates were computed in the previous section. Accordingly the dc conductivity is given, up to logarithmic corrections, by

$$\sigma_{\rm dc} \simeq \frac{1}{T}(\Gamma_{\rm sp} + \Gamma_{\rm int}), \tag{15}$$

and its overall temperature dependence is nonmonotonic: it transitions from activated behavior at $T \gtrsim W_s \ln(W_c/W_s)$ to a $1/T$ growth at lower temperatures down to $T \sim W_s$. At still lower temperatures, presumably the dc conductivity vanishes again, but this is outside the regime of validity of our analysis (this regime is explored, e.g., in Ref. [53]). The various regimes are plotted in Fig. 2.

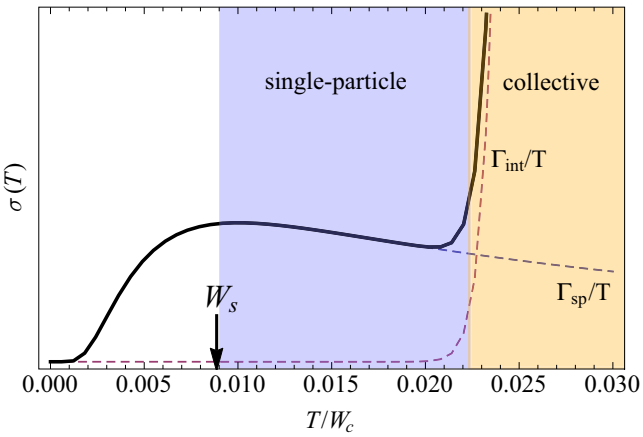

FIG. 2. Low-temperature dc charge conductivity $\sigma(T)$ (in arbitrary units) of strongly interacting spinful chains, plotted for parameters $W_s = 0.01 W_c$, $\xi_p = 10$, and $\xi_q = 5$. At relatively high temperatures in the SILL regime [i.e., $W_s \ln(W_c/W_s) \lesssim T \lesssim W_c$], the dominant contribution to $\sigma(T)$ comes from collective rearrangements, and is activated (beige region). At relatively low temperatures in the SILL regime [i.e., $W_s \lesssim T \lesssim W_s \ln(W_c/W_s)$], single-particle hops dominate, and $\sigma(T) \sim 1/T$ (blue region). The thick line shows the total dc conductivity (15); the single-particle and collective contributions are plotted as dashed lines, given by $\Gamma_{\rm sp}/T$ and $\Gamma_{\rm int}/T$, respectively, with the relevant relaxation rates given by (12) and (13). The behavior of $\sigma(T)$ at still lower temperatures, $T < W_s$ (i.e., in the spinful Luttinger-liquid regime rather than the SILL regime), is outside the scope of this work. We expect that the conductivity here is due to conventional hopping mechanisms and drops rapidly to zero. An appreciable regime of nonmonotonic behavior exists when $\ln(W_c/W_s) \gg 1$, i.e., whenever there is a well-defined SILL regime.

VI. ENERGY TRANSPORT

Three separate channels exist for energy transport: the charge carriers (instantons) discussed in the previous section, spins, and neutral phononlike excitations. The energy carried by spin and charge carriers is straightforward to estimate, but the contribution due to phonons is more nontrivial. In this section, we discuss the first two of these, then estimate the phonon contribution. Comparing the three then permits us to establish regimes in which each is dominant.

A. Spin- and charge-based contributions

Spin excitations diffuse with a diffusion constant $\mathcal{D} \sim W_s$; since their energy is bandwidth-limited, for $T \gg W_s$ each such excitation carries $Q \sim W_s$ of energy. The typical thermal density of states for a spin excitation is $n_s(T) \sim e^{-W_s/T}$; using the Einstein relation for a thermal gradient, we find

$$\kappa_s(T) \sim Q^2 \mathcal{D} \frac{\partial n_s}{\partial T} \underset{T \gg W_s}{\sim} \frac{W_s^3}{T^2}. \tag{16}$$

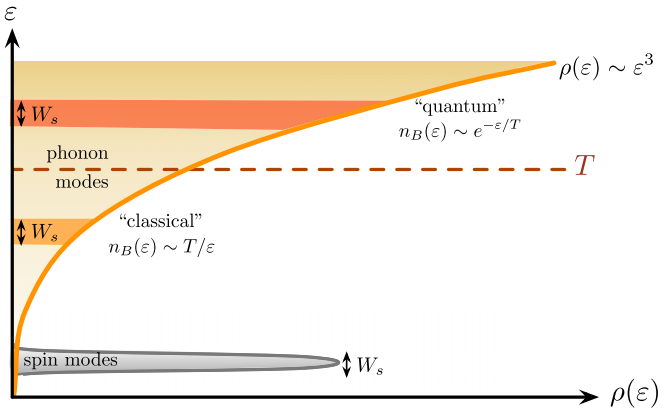

FIG. 3. "Foliated" phonon density of states. Owing to the narrow bandwidth W_s of the spin modes, spin-flip assisted boson hopping can only occur within a narrow "shell" of width W_s. This "foliation" leads to an emergent approximate conservation law for phonons within a particular shell. Phonons in shells centered at energy $\varepsilon \ll T$ ($\varepsilon \gg T$) are effectively classical (quantum), with occupancy $n_B(\varepsilon) \sim T/\varepsilon$ [$n_B(\varepsilon) \sim e^{-\varepsilon/T}$].

The charge-transport contribution to the energy conductivity is related to the charge conductivity (15) by a Wiedemann-Franz law,

$$\kappa_{\text{inst}} \simeq \sigma_{\text{dc}} T; \tag{17}$$

thus it is activated at high temperatures and *constant* at low temperatures. [More precisely, this contribution has a plateau for temperatures such that $W_s \lesssim T \lesssim W_s \ln(W_c/W_s)$. At still lower temperatures, our SILL-based description does not apply, and on general grounds we expect the thermal conductivity to decrease rapidly to zero (Fig. 2).]

B. "Foliated" variable-range hopping for phonons

Phonons are not conserved, so in most contexts it does not make sense to talk about their *hopping* conductivity. A peculiarity of the present system, which makes phonon hopping a physically relevant channel, is the $W_s \ll T$ limit. In this limit, phonons with energy $\gtrsim W_s$ cannot be created or destroyed at low order in the spin-charge coupling. Such phonons are extremely rare due to the vanishing phonon density of states at zero energy. Instead, the dominant phonons (which have energy $\sim T$) hop among modes that are separated by $\lesssim W_s$. Thus the space of phonons is "foliated" (Fig. 3); each phonon hop transfers $\sim W_s$ of energy between the spin and phonon sectors, while moving a much larger amount of energy $\sim T$ between two spatially separated localized phonon orbitals. To a good approximation (i.e., up to an energy resolution $\sim W_s$) we can consider each "foliation" separately.[4] The effective thermal conductance between two localized bosonic states i, j located R_i, R_j and belonging to the same foliation (i.e., for $\varepsilon_i \sim \varepsilon_j \sim \varepsilon$ to precision W_s) is given by (see Appendix for details)

$$K_{ij}(\varepsilon) \sim \frac{g^2}{W_s}\frac{\varepsilon^2}{T^2} e^{-\frac{2|R_i - R_j|}{\xi_p}} n_B(\varepsilon)[1 + n_B(\varepsilon)], \tag{18}$$

where we have taken the spin-flip density of states (assumed constant) to be $\nu_s^0 \sim 1/W_s$, g is again the spin-charge coupling, $\xi_{\text{eff}}(\varepsilon)$ is the effective localization length at energy ε, and we drop prefactors of order one. As noted above, the foliation of the energy spectrum leads to an approximate conservation law: there is little energy transfer between the different bands, so that we may simply consider a set of distinct hopping problems, and argue that the one with the largest thermal conductance dominates the rest. Within each energy window, the problem thus reduces to determining the effective thermal conductance of the random thermal resistor network with resistances K_{ij}^{-1}. The broad distribution of the K_{ij}s (even at a fixed energy ε) permits us to argue that the scaling of the effective phonon thermal conductivity κ_{ph} is given by the critical K_c at the percolation threshold; bonds with $K_{ij} > K_c$ fail to percolate and cannot contribute to the conductance across the whole sample, whereas those with $K_{ij} < K_c$ are shorted out by the percolating backbone. This procedure can be implemented numerically quite straightforwardly; however, we eschew this in favor of an analytical estimate that is sufficient to obtain the scaling of K with temperature.

Before proceeding, we must estimate the typical real-space distance between bosonic modes at energy ε. The density of states of these modes may be approximated as $\rho(\varepsilon) \approx \frac{1}{cW_c}(\frac{\varepsilon}{W_c})^3$ where c is an $O(1)$ constant; from this, we see that the typical spacing between levels in the energy window $(\varepsilon, \varepsilon + W_s)$ is given by $R_{\text{eff}}(\varepsilon) \sim c\frac{W_c}{W_s}(\frac{W_c}{\varepsilon})^3$. Thus we may rewrite (18) as

$$K_{ij}(\varepsilon) \sim \frac{g^2}{W_s}\frac{\varepsilon^2}{T^2} e^{-c[{W_c}^4/(\varepsilon^3 W_s)]} n_B(\varepsilon)[1 + n_B(\varepsilon)], \tag{19}$$

where we have absorbed all numerical factors in the exponent by redefining the constant c. The Bose factors that enter the expression for $K_{ij}(\varepsilon)$ simplify in two limits: the "classical" case when $\varepsilon \ll T$, and the "quantum" case when $\varepsilon \gg T$. We now discuss each in turn.

1. Classical Regime

In the classical regime, we have $n_B(\varepsilon) \approx T/\varepsilon \gg 1$, so that the typical thermal conductance of a foliation around ε is

$$K_{ij}^{\text{cl}}(\varepsilon) \sim \frac{g^2}{W_s} e^{-c[{W_c}^4/(\varepsilon^3 W_s \xi_p)]} \tag{20}$$

and we assume this form is valid up to $\varepsilon \sim T$, where the classical-quantum crossover occurs. Clearly, the states with $\varepsilon \ll T$ will have extremely suppressed conductances, so that the dominant classical channel is obtained right at the crossover scale. Note that the classical processes are not really "variable range:" there is no tradeoff between distance and energy, and

[4] One might expect that the small changes in energy involved in each hopping process would lead any particular phonon to "diffuse" out of its initial foliation after a number of hops, while others diffuse in. However, transitions into modes that are very far from the optimal foliation (e.g., a series of downhill transitions) strongly diminish the mobility of the phonon. The dominant transport paths are those in which a phonon hops among modes that belong to the optimal foliation.

hopping always occurs to the nearest neighbor site within the same foliation. The corresponding thermal conductivity is

$$\kappa_{\rm ph}^{\rm cl} \sim \frac{g^2}{W_s} e^{-c[W_c{}^4/(\varepsilon^3 W_s \xi_p)]}. \tag{21}$$

This is subleading relative to the contribution from the quantum channels (see below).

2. *Quantum regime*

In the quantum regime, we have $n_B(\varepsilon) \approx e^{-\varepsilon/T} \ll 1$, leading to a typical conductance

$$K_{ij}^{\rm q}(\varepsilon) \sim \frac{g^2}{W_s} \frac{\varepsilon^2}{T^2} e^{-c[W_c{}^4/(\varepsilon^3 W_s \xi_p)]-\varepsilon/T}. \tag{22}$$

We optimize the exponent among the classical channels with $\varepsilon \gg T$, and find that the dominant channel is at the energy

$$\varepsilon_c = W_c \left(\frac{3cT}{W_s \xi_p} \right)^{1/4}. \tag{23}$$

The expression (23) is only meaningful if $\varepsilon_c \lesssim W_c$, which is the case when $cT \lesssim W_s \xi_p$ (i.e., for relatively low temperatures in systems with relatively weak disorder). In this regime, the thermal conductivity from the dominant channel is

$$\kappa_{\rm ph}^{\rm q}(T) \sim \frac{g^2}{W_s} a \frac{W_c^2}{\sqrt{W_s T^3}} e^{-bW_c/(\xi_p W_s T^3)^{1/4}} \tag{24}$$

with $a = (3c/4)^{1/2}$ and $b = 7/3(3c/4)^{1/4}$. Note that this dominates the classical contribution (21). In the opposite limit of small ξ_p or high T, the dominant channels are those at the highest available energies $\sim W_c$. The temperature dependence in this limit is *activated*, although the precise rate is outside the scope of the present work (as the relevant modes are not in the SILL regime). Therefore we conclude that the thermal conductance due to phonons is given by Eq. (24), provided that the temperature is low and ξ_p is large.

So far, in this analysis, we have assumed that single-phonon hops dominate over multi-phonon rearrangements. This assumption holds because the dominant phonon channels (as computed above) have energies that are much higher than T. Therefore such excitations are sufficiently dilute that interaction effects are expected to be subleading.

C. Evolution of κ with temperature

The three contributions to thermal conductivity at temperature T are listed in Eqs. (16), (17), and (24). The overall temperature dependence of $\kappa(T)$ implied by these is as follows. At temperatures that are not much larger than W_s, the thermal conductivity is dominated by spin excitations, which propagate *fastest* but carry the least energy per excitation. At higher temperatures, i.e., at temperatures close to W_c, the other channels can in principle dominate because each excitation in these channels (though slower-moving) carries more energy $\gtrsim T$. In general, there will be a crossover between spin and phonon channels at a temperature set by

$$\frac{W_s^3}{(T^*)^2} \sim \frac{g^2}{W_s} a \frac{W_c^2}{\sqrt{W_s (T^*)^3}} e^{-bW_c/(\xi_p W_s (T^*)^3)^{1/4}}. \tag{25}$$

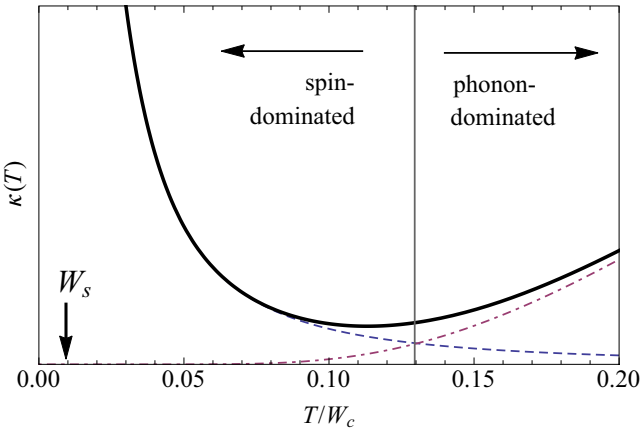

FIG. 4. Thermal conductivity (in arbitrary units) in the SILL regime, plotted for parameters $W_s = 0.01W_c$, $g = 0.1W_s$, and $\xi_p = 10$. For these parameters, the instanton contribution is always subleading; instead, there is a crossover from phonon-mediated energy transport [dash-dotted line, $\kappa_{\rm ph}^{\rm q}(T)$ in (24)] at relatively high temperatures to spin-mediated energy transport at relatively low temperatures [dashed line, $\kappa_{\rm s}(T) \sim W_s^3/(W_s^2 + T^2)$, as appropriate to spin diffusion for $T \gg W_s$ crossing over to low-temperature behavior as $T \to 0$]. The thick line shows the behavior of the total thermal conductivity $\kappa = \kappa_{\rm ph}^{\rm q} + \kappa_{\rm s}$, that peaks at $T \sim W_s$. At temperatures below W_s, the thermal conductivity should decrease and $\kappa(T \to 0) = 0$; we do not discuss the details of this behavior here as it lies outside the SILL regime. For stronger disorder or weaker spin-charge coupling, the crossover temperature T^* [gray vertical line, given by (25)] increases.

This equation has *no* solutions for $W_s \lesssim T \lesssim W_c$ unless ξ_p is sufficiently large; however, for sufficiently large ξ_p (i.e., weak disorder) there is a temperature regime in which the phonons dominate over the spins. Analogous estimates suggest that instantons never dominate energy transport, as they are always subleading either to spins or to phonons. The resulting crossover is shown in Fig. 4: in general, the dc thermal conductivity has a *minimum* at temperatures between W_s and W_c, because at these temperatures the charge degrees of freedom are essentially frozen out whereas the spin degrees of freedom contribute weakly to response because they are at infinite temperature.

D. Finite-frequency thermal conductivity

Finally, we briefly remark on the ac thermal conductivity at finite temperature. We expect this to be dominated by phonons, because they are much more weakly localized than instantons (assuming $\xi_q \ll \xi_p$). Let us again assume that $W_s \ll \omega \ll T$; thus the spin sector does not respond and can be neglected. The "foliated" analysis of the previous sections can be reprised but with ω playing the role of W_s. Thus ω determines a length-scale $x_\omega = \xi_p \ln(W_c/\omega)$. Consider a particular foliation centered at energy ε. The spacing between states in this foliation is $r_\varepsilon \sim W_c^4/(W_s \varepsilon^3)$, and the fraction of occupied states is $\exp(-\varepsilon/T)$. Thus the ac thermal conductivity from a particular foliation is

$$\kappa_\varepsilon(\omega) = T(\omega r_\omega)^2 \exp(-\varepsilon/T) r_\omega/(W_c r_\varepsilon). \tag{26}$$

This is maximized for $\varepsilon \sim T$, and so the ac thermal conductivity goes (up to logs) as

$$\kappa(\omega, T) \sim \omega^2 T^4. \tag{27}$$

VII. DISCUSSION

We have argued that the concept of "superuniversality" breaks down for the dynamics of isolated spin-incoherent Luttinger liquids in the presence of disorder. Instead, the spin exchange time scale governs charge and energy dynamics. We have estimated the charge and energy conductivities and shown that they exhibit multiple regimes: charge transport at relatively high temperatures is due to many-body resonances, whereas at low temperatures (but still in the SILL regime) it is due to single-particle hops. Energy transport, meanwhile, is due to spin excitations at low temperatures and (for sufficiently weak disorder) due to phonons (collective charge modes) at higher temperatures. Both transport coefficients evolve *nonmonotonically* with temperature in the SILL regime (Figs. 2 and 4).

Our results generalize readily to interacting two-component systems under the following conditions: (i) one of the components has a much smaller intrinsic energy scale (i.e., bandwidth) than the other, but is also subject to much weaker disorder; and (ii) the coupling between the two components is weak compared with the intrinsic energy scale of either.

In the case of the SILL, which we have focused on so far, condition (i) is guaranteed by strong interactions whereas condition (ii) is a consequence of spin-charge separation. However, similar two-component systems can also be implemented, e.g., using two-leg ladders [54,55], working with two or more species of particles with a large mass ratio [56], or using weak transverse hopping in lieu of the "spin" [13]. Existing finite-size numerical studies of such systems [54,57] are qualitatively consistent with our conclusions; however, these are reliable in the *strongly disordered* limit, whereas our calculations are most controlled in the complementary limit of *weak* disorder.

Our results apply directly to a number of spinful solid-state systems, with predominantly short-range exchange coupling, as well as to ultracold atomic gases [58]. However, for experiments with semiconductor nanowires [59–61], some of our results will be modified because of the power-law tail of the Coulomb interaction. In particular, rather than being exponentially localized, phonons will only be power-law localized (with tails falling off as [62] $1/x^3$). One expects the dc conductivity in this regime to go as a power-law of the temperature, with the exponents depending on the observable as well as the power-law of the interaction: for instance, for Coulomb interacting electrons in 1D the dc charge conductivity $\sigma_{\rm dc} \sim T^2 W_s^3 / W_c^5$. Since our predictions involve transport, they can be tested by standard conductivity measurements in solid-state settings [59,60]. Our predictions are straightforward to test in transport experiments or quench dynamics involving ultracold atoms [41,63,64]: the predictions for energy transport can be explored in cold atomic systems, e.g., using the local thermometry scheme in Ref. [65]. Using this method, the ac thermal conductivity can also be extracted from the time-dependent autocorrelation function of the energy density.

We now briefly discuss how our results are modified when conditions (i) and (ii) above fail. First, we consider the failure of condition (ii): for instance, in the two-leg ladders of Refs. [54,55], or in the SILL at relatively strong disorder, where spin and charge are not cleanly separated. In this case, a crucial distinction exists between systems in which the full Hamiltonian obeys SU(2) symmetry and those in which it does not, e.g., generic two-component systems or spin-orbit coupled systems. In the absence of SU(2) symmetry, the charge sector can *localize* the spin sector [46], so that the full system exhibits a form of asymptotic many-body localization [55,66] (although it is unclear at present whether such asymptotic localization is stable against rare-region effects [67,68]). On the other hand, in the presence of SU(2) symmetry, it appears [35,69] that the spin sector is protected against many-body localization. Thus we expect our analysis to extend to the case of intermediate or strong spin-charge coupling for SU(2) symmetric systems, at least qualitatively. However, our treatment of the spin sector as being thermal but otherwise featureless might fail here. For instance, equilibrium spatial fluctuations in the charge density will lead to large spatial fluctuations in W_s, and regions of anomalously small W_s might act as bottlenecks for hopping transport as discussed in Ref. [70].

Finally, we comment on the crossover between the strongly interacting systems considered here and the weakly interacting limit of Refs. [8,9] (note that Ref. [8], like most of the extant literature, considered spinless fermions). For concreteness we consider the Hubbard model, and ignore spin-orbit coupling. In the noninteracting disordered problem, all orbitals are localized; the N-particle ground state (for even particle number) involves doubly occupying the lowest $N/2$ orbitals, and has no spin degeneracy. However, a state at finite energy density generically has a number of singly occupied orbitals, each of which is spin degenerate. For weak interactions, exchange interactions lift these spin degeneracies. If one imagines "freezing" the charges in a particular configuration of orbitals, the resulting spin Hamiltonian will have random exchange couplings (inherited from the positional randomness of the orbitals) but will, crucially, respect SU(2) symmetry. This symmetry prevents localization in the spin sector. Thus, spins will thermalize even in this putative fixed charge background, and will thermalize the charges as well. In this low-temperature limit, the density of singly occupied orbitals goes as $T/E_F \sim T/W_c$; consequently the exchange coupling between them (which sets the bandwidth of the spin bath) will go as $U \exp(-(E_F/T)/\xi)$ where ξ is the single-particle localization length. Thus the physics of relaxation through a narrow-bandwidth spin bath also applies in the weak-coupling regime. However, the charge and spin temperatures are essentially the same at weak coupling (as $W_c \simeq W_s$), so the unusual nonmonotonic transport signatures discussed in this work will not be present there. Figure 5 summarizes the various regimes.

In closing, we observe that, for reasons described in Sec. III, the disordered, isolated SILL is *not* a many-body localized system. It has two intrinsic channels for thermalization, viz. the spin bath that we have focused on, as well as the high-energy

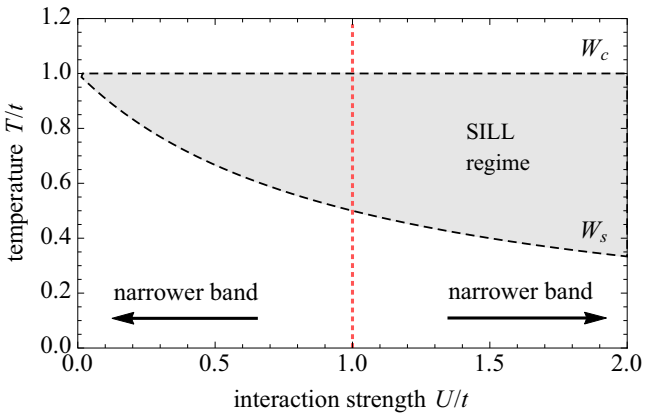

FIG. 5. Evolution of the SILL regime (shaded), and the characteristic bandwidth of the spin bath, for the disordered Hubbard model in one dimension. As interactions increase, the spin and charge bandwidths W_c, W_s separate and an intermediate temperature regime (i.e., the SILL regime) opens up. The effective bandwidth of the spin bath, which mediates charge relaxation, is governed by U at weak coupling and by t^2/U at strong coupling; thus it becomes narrow (and the relaxation time scales diverge) in both limits.

charge modes, which are thermal in the strongly interacting, weakly disordered limit where our calculations are controlled. Thus the SILL is in fact an ergodic system—for instance, we expect that its eigenstates are volume-law entangled, and that observables computed in single eigenstates at finite energy density will exhibit thermal behavior. Nevertheless, we have shown that the transport and dynamics show many features that are most easily understood by beginning with an MBL system and adding perturbations that thermalize it. In this sense, the SILL provides a new example of a thermal system whose dynamics are fruitfully addressed from the MBL perspective. We anticipate that there are other situations where such phenomenology emerges, and that similar "MBL-controlled" crossovers may be surprisingly ubiquitous, particularly in low-dimensional disordered systems.

ACKNOWLEDGMENTS

We thank M. Babadi, B. Bauer, A. L. Chernyshev, T. Grover, D. A. Huse, F. Huveneers, M. Knap, I. Lerner, R. Nandkishore, V. Oganesyan, A. C. Potter, and S. L. Sondhi for helpful discussions. We also acknowledge two anonymous referees for valuable comments on pedagogy. This research was supported in part by the National Science Foundation under Grants No. NSF PHY11-25915 at the KITP (S.A.P., S.G.) and CAREER Award DMR-1455366 (S.A.P.). S.G. acknowledges support from the Burke Institute at Caltech. We acknowledge the hospitality of the KITP and highways US-101, CA-134, CA-118, and CA-126, where portions of this work were carried out.

APPENDIX: PHONON VARIABLE-RANGE HOPPING

In this appendix, we provide details of of the Gaussian-sector VRH calculation. As in the main text, we consider a set of localized bosonic modes at random positions i, with random energies $\varepsilon_i > 0$ (the positivity of constraint is because the Gaussian sector describes excitations above the pinned CDW ground state), distributed according to the density of states $\rho(\varepsilon)$.

The change in the distribution function of level 1 due to transitions to and from level 2 is obtained from Fermi's golden rule as

$$\partial_t n(\varepsilon_1) = 2\pi g^2 e^{-2|R_i-R_j|/\xi_p} \sum_\mu \{\delta(\varepsilon_1-\varepsilon_2-E_\mu)[(1+n_B(\varepsilon_1))n_B(\varepsilon_2)n_B(E_\mu) - n_B(\varepsilon_1)(1+n_B(\varepsilon_2))(1+n_B(E_\mu))]$$
$$+\delta(\varepsilon_1+\varepsilon_2-E_\mu)[(1+n_B(\varepsilon_1))n_B(\varepsilon_2)n_B(-E_\mu) - n_B(\varepsilon_1)(1+n_B(\varepsilon_2))(1+n_B(-E_\mu))]\}, \quad \text{(A1)}$$

where μ indexes all the single-spin-flip processes in the first expression we have approximated a common matrix element $|\mathcal{H}_{\text{el-s}}|^2 \approx g^2 e^{-2|R_i-R_j|/\xi_p}$ for all single-spin-flip processes involving bosons localized on sites i, j, where ξ_p is the pinning length.

We may perform the sum over μ by converting into an integral $\sum_\mu(\ldots) \to \int_0^\infty d\varepsilon \nu_s(\varepsilon)(\ldots)$ where $\nu_s(\varepsilon)$ is the density of states of the spin-flip processes. From this, we obtain a general formula for the transition rate from state i to state j,

$$\Gamma^0_{ij}(\varepsilon_i,\varepsilon_j,R_i,R_j) = 2\pi g^2 e^{-2|R_i-R_j|/\xi_p} \nu_s(|\varepsilon_i-\varepsilon_j|) n_B(\varepsilon_i)(1+n_B(\varepsilon_j)) \begin{cases} \tilde{n}_B(\varepsilon_j-\varepsilon_i), & \varepsilon_i < \varepsilon_j \\ 1+\tilde{n}_B(\varepsilon_i-\varepsilon_j), & \varepsilon_i > \varepsilon_j. \end{cases}$$
$$\equiv n_B(\varepsilon_i)(1+n_B(\varepsilon_j))\gamma^0_{ij}(\varepsilon_i,\varepsilon_j,R_i,R_j). \quad \text{(A2)}$$

where we have separated out the occupancy factors from the "intrinsic" transition rate γ^0_{ij}. The occupation factors $\tilde{n}_B$ for the spin-sector excitations are taken to be those of strongly anharmonic bosonic modes, i.e., the thermal occupation of each spin mode is truncated at a number on the order of unity. It is readily verified that these rates satisfy the detailed balance condition $\Gamma^0_{ij} = \Gamma^0_{ji}$, required to define equilibrium in the absence of temperature and field gradients. As a next step, we need to relate the thermal conductivity to the equilibrium hopping rate Γ^0_{ij}. To that end, we imagine

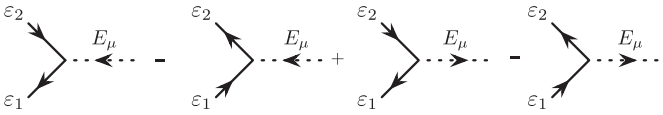

FIG. 6. Diagrams for one-spin-flip absorption and emission processes that contribute to the transition rate for localized bosonic states.

imposing a temperature gradient ∇T, so that the sites i and j are at different temperatures. While this shifts the occupancy factors by adjusting the local temperature at sites i,j, there is no change in the intrinsic transition rate γ^0_{ij}. This is a consequence of the Bose factors entering γ^0_{ij} reflect the occupancy of the spin-flip mode absorbed or emitted to make up the energy difference between $\varepsilon_i,\varepsilon_j$; since the characteristic energy scale $|\varepsilon_i-\varepsilon_j|$ is set by the maximal spin-flip energy $\sim W_s$ and we have $T \gg W_s$, small variations in the temperature over distance $\sim\xi_{\rm eff}$ may be ignored, so that we may simply compute γ^0_{ij} at the average temperature of sites i,j, namely, T. Under these assumptions, the differential rate for boson hopping between sites i and j is obtained as (putting explicit temperature dependence in the occupancy factors to reflect the thermal gradient)

$$\begin{aligned}\Delta\Gamma_{ij}(\nabla T) &\equiv \Gamma_{ij}(\varepsilon_i,\varepsilon_j,R_i,R_j)|_{\nabla T} - \Gamma_{ji}(\varepsilon_i,\varepsilon_j,R_i,R_j)|_{\nabla T}\\ &= \gamma^0_{ij}(\varepsilon_i,\varepsilon_j,R_i,R_j)n_B(\varepsilon_i,T_i)(1+n_B(\varepsilon_j,T_j))\\ &\quad -\gamma^0_{ji}(\varepsilon_i,\varepsilon_j,R_i,R_j)n_B(\varepsilon_j,T_j)(1+n_B(\varepsilon_i,T_i))\\ &= \Gamma^0_{ij}\left[\frac{\delta n_i}{n^0_i(1+n^0_i)} - \frac{\delta n_j}{n^0_j(1+n^0_j)}\right], \end{aligned} \tag{A3}$$

where we have defined $n^0_i \equiv n_B(\varepsilon_i,T)$, and $\delta n_i \equiv n_B(\varepsilon_i,T_i) - n^0_B$. Assuming the linear-response regime, we may take $T_{i,j} \approx T \pm \frac{\vec{R}_{ij}}{2}\cdot\vec{\nabla}T \equiv T \pm \frac{\delta T}{2}$, where $\vec{R}_{ij} \equiv R_i - R_j$. With this parametrization, we have, after a little work,

$$\Delta\Gamma_{ij}(\nabla T) = \frac{\varepsilon_i+\varepsilon_j}{2T^2}\Gamma^0_{ij}\times(\vec{R}_{ij}\cdot\vec{\nabla}T). \tag{A4}$$

In order to obtain the energy current, we must multiply this number current by the typical energy transported in the tunneling process, which we take to be the average energy of sites i,j, yielding

$$I^{(Q)}_{ij} = \frac{(\varepsilon_i+\varepsilon_j)^2}{4T^2}\Gamma^0_{ij}\times(\vec{R}_{ij}\cdot\vec{\nabla}T). \tag{A5}$$

Note that the expression in parentheses is the net temperature difference between the two sites; thus, the remainder of the RHS of (A5) is the thermal conductance between sites i,j,

$$K_{ij} = \frac{(\varepsilon_i+\varepsilon_j)^2}{4T^2}\Gamma^0_{ij}(\varepsilon_i,\varepsilon_j,R_i,R_j). \tag{A6}$$

Two observations allow us to simplify the expression above. First, in the usual electron variable-range-hopping computation, the density of hopping levels $\rho(\varepsilon)$ is treated as roughly constant, in contrast to the scaling $\rho(\varepsilon)\sim\varepsilon^\gamma$ appropriate to the quantized Gaussian fluctuations of the CDW. Second, the phonon bath invoked in those treatments is assumed to be able to absorb and emit at any frequency: the "perfect bath" limit. In essence, this allows us to take $|\varepsilon_i-\varepsilon_j| \gg T$ when computing the intrinsic rate. Here, in contrast, we have a narrow bath, and therefore the spin-flip density of states vanishes for large energy differences $|\varepsilon_i-\varepsilon_j| \gtrsim W_s$, and we are working in the regime where $W_s \ll T$. As a consequence, Γ^0_{ij} vanishes unless $|\varepsilon_i-\varepsilon_j| \lesssim W_s$; since $\rho(\varepsilon)\sim\varepsilon^\gamma$ over a range $W_c \gg W_s$, it follows that we must consider a sequence of VRH problems within energy bands of width W_s and with a density of localized states given by ρ_s. In other words, this is the "foliation" discussed in the main text: since $\nu_s(\varepsilon_i-\varepsilon_j) \approx \frac{1}{W_s}\Theta(W_s-|\varepsilon_i-\varepsilon_j|)$, both levels $\varepsilon_i,\varepsilon_j$ are at approximately the same energy (within the resolution of the bath bandwidth) for all the factors on the RHS. As a consequence, within the energy resolution W_s, we may approximate Γ^0_{ij} by a hopping rate that depends on a single energy ε,

$$\Gamma^0_{ij} \approx 2\pi g^2\nu^0_s e^{-\frac{2|R_i-R_j|}{\xi_p}} n_B(\varepsilon)[1+n_B(\varepsilon)], \tag{A7}$$

whence we find that the thermal conductance between i,j is

$$K_{ij}(\varepsilon) \approx 2\pi g^2\nu^0_s\frac{\varepsilon^2}{T^2}e^{-\frac{2|R_i-R_j|}{\xi_p}} n_B(\varepsilon)[1+n_B(\varepsilon)]. \tag{A8}$$

[1] A. Berkovich, J. Phys. A **24**, 1543 (1991).
[2] V. V. Cheianov and M. B. Zvonarev, Phys. Rev. Lett. **92**, 176401 (2004).
[3] K. A. Matveev, Phys. Rev. Lett. **92**, 106801 (2004).
[4] G. A. Fiete and L. Balents, Phys. Rev. Lett. **93**, 226401 (2004).
[5] G. A. Fiete, Rev. Mod. Phys. **79**, 801 (2007).
[6] F. D. M. Haldane, J. Phys. C **14**, 2585 (1981).
[7] T. Giamarchi, *Quantum Physics in One Dimension* (Clarendon Press, Oxford, 2004).
[8] D. Basko, I. Aleiner, and B. Altshuler, Ann. Phys. **321**, 1126 (2006).
[9] I. V. Gornyi, A. D. Mirlin, and D. G. Polyakov, Phys. Rev. Lett. **95**, 206603 (2005).
[10] V. Oganesyan and D. A. Huse, Phys. Rev. B **75**, 155111 (2007).
[11] R. Nandkishore and D. A. Huse, Ann. Rev. Condens. Matter Phys. **6**, 15 (2015).
[12] E. Altman and R. Vosk, Annu. Rev. Condens. Matter Phys. **6**, 383 (2015).
[13] P. Bordia, H. P. Lüschen, S. S. Hodgman, M. Schreiber, I. Bloch, and U. Schneider, Phys. Rev. Lett. **116**, 140401 (2016).
[14] S. Gopalakrishnan and R. Nandkishore, Phys. Rev. B **90**, 224203 (2014).
[15] Y. Bar Lev, G. Cohen, and D. R. Reichman, Phys. Rev. Lett. **114**, 100601 (2015).
[16] K. Agarwal, S. Gopalakrishnan, M. Knap, M. Müller, and E. Demler, Phys. Rev. Lett. **114**, 160401 (2015).
[17] R. Vosk, D. A. Huse, and E. Altman, Phys. Rev. X **5**, 031032 (2015).

[18] A. C. Potter, R. Vasseur, and S. A. Parameswaran, Phys. Rev. X **5**, 031033 (2015).
[19] D. J. Luitz, N. Laflorencie, and F. Alet, Phys. Rev. B **93**, 060201 (2016).
[20] G. A. Fiete, K. Le Hur, and L. Balents, Phys. Rev. B **72**, 125416 (2005).
[21] S. V. Malinin, T. Nattermann, and B. Rosenow, Phys. Rev. B **70**, 235120 (2004).
[22] B. Rosenow and T. Nattermann, Phys. Rev. B **73**, 085103 (2006).
[23] T. Giamarchi and H. J. Schulz, Phys. Rev. B **37**, 325 (1988).
[24] A. I. Larkin and P. A. Lee, Phys. Rev. B **17**, 1596 (1978).
[25] M. V. Feigel'man, Sov. Phys. JETP **52**, 555 (1980).
[26] M. V. Feigel'man and V. M. Vinokur, Phys. Lett. A **87**, 53 (1981).
[27] T. Nattermann, T. Giamarchi, and P. Le Doussal, Phys. Rev. Lett. **91**, 056603 (2003).
[28] Z. Ristivojevic, A. Petković, P. Le Doussal, and T. Giamarchi, Phys. Rev. Lett. **109**, 026402 (2012).
[29] G. Refael and E. Altman, C. R. Phys. **14**, 725 (2013), disordered systems/Systèmes désordonnés.
[30] M. M. Fogler and E. Pivovarov, Phys. Rev. B **72**, 195344 (2005).
[31] J. S. Meyer and K. A. Matveev, J. Phys.: Condens. Matter **21**, 023203 (2008).
[32] Y. Imry and S.-k. Ma, Phys. Rev. Lett. **35**, 1399 (1975).
[33] A. D. Mirlin, D. G. Polyakov, and V. M. Vinokur, Phys. Rev. Lett. **99**, 156405 (2007).
[34] S. Banerjee and E. Altman, Phys. Rev. Lett. **116**, 116601 (2016).
[35] R. Vasseur, A. C. Potter, and S. A. Parameswaran, Phys. Rev. Lett. **114**, 217201 (2015).
[36] A. V. Andreev, S. A. Kivelson, and B. Spivak, Phys. Rev. Lett. **106**, 256804 (2011).
[37] A. J. Leggett, S. Chakravarty, A. T. Dorsey, M. P. A. Fisher, A. Garg, and W. Zwerger, Rev. Mod. Phys. **59**, 1 (1987).
[38] M. M. Fogler, Phys. Rev. Lett. **88**, 186402 (2002).
[39] R. Modak and S. Mukerjee, Phys. Rev. Lett. **115**, 230401 (2015).
[40] X. Li, S. Ganeshan, J. H. Pixley, and S. Das Sarma, Phys. Rev. Lett. **115**, 186601 (2015).
[41] S. Gopalakrishnan, M. Müller, V. Khemani, M. Knap, E. Demler, and D. A. Huse, Phys. Rev. B **92**, 104202 (2015).
[42] J. Z. Imbrie, J. Stat. Phys. **163**, 998 (2016).
[43] M. Serbyn, Z. Papić, and D. A. Abanin, Phys. Rev. X **5**, 041047 (2015).
[44] L. Rademaker and M. Ortuño, Phys. Rev. Lett. **116**, 010404 (2016).
[45] D. Abanin, W. De Roeck, and F. Huveneers, arXiv:1412.4752 [cond-mat.dis-nn].
[46] R. Nandkishore, Phys. Rev. B **92**, 245141 (2015).
[47] V. Ambegaokar, B. I. Halperin, and J. S. Langer, Phys. Rev. B **4**, 2612 (1971).
[48] B. I. Shklovskii and A. L. Efros, *Electronic Properties of Doped Semiconductors* (Springer Science+Business Media, New York, 2013), Vol. 45.
[49] N. F. Mott, Philos. Mag. **17**, 1259 (1968).
[50] S. Gopalakrishnan, M. Knap, and E. Demler, Phys. Rev. B **94**, 094201 (2016).
[51] M. Kozarzewski, P. Prelovsek, and M. Mierzejewski, Phys. Rev. B **93**, 235151 (2016).
[52] J. Rehn, A. Lazarides, F. Pollmann, and R. Moessner, Phys. Rev. B **94**, 020201 (2016).
[53] A. G. Yashenkin, I. V. Gornyi, A. D. Mirlin, and D. G. Polyakov, Phys. Rev. B **78**, 205407 (2008).
[54] K. Hyatt, J. R. Garrison, A. C. Potter, and B. Bauer, arXiv:1601.07184.
[55] N. Y. Yao, C. R. Laumann, J. I. Cirac, M. D. Lukin, and J. E. Moore, Phys. Rev. Lett. **117**, 240601 (2016).
[56] T. Grover and M. P. A. Fisher, J. Stat. Mech. (2014) P10010.
[57] R. Mondaini and M. Rigol, Phys. Rev. A **92**, 041601 (2015).
[58] G. Pagano, M. Mancini, G. Cappellini, P. Lombardi, F. Schafer, H. Hu, X.-J. Liu, J. Catani, C. Sias, M. Inguscio, and L. Fallani, Nat. Phys. **10**, 198 (2014).
[59] O. Auslaender, H. Steinberg, A. Yacoby, Y. Tserkovnyak, B. Halperin, K. Baldwin, L. Pfeiffer, and K. West, Science **308**, 88 (2005).
[60] H. Steinberg, O. M. Auslaender, A. Yacoby, J. Qian, G. A. Fiete, Y. Tserkovnyak, B. I. Halperin, K. W. Baldwin, L. N. Pfeiffer, and K. W. West, Phys. Rev. B **73**, 113307 (2006).
[61] D. Laroche, G. Gervais, M. P. Lilly, and J. L. Reno, Science **343**, 631 (2014).
[62] N. Y. Yao, C. R. Laumann, S. Gopalakrishnan, M. Knap, M. Müller, E. A. Demler, and M. D. Lukin, Phys. Rev. Lett. **113**, 243002 (2014).
[63] M. Pasienski, D. McKay, M. White, and B. DeMarco, Nat. Phys. **6**, 677 (2010).
[64] S. Krinner, D. Stadler, J. Meineke, J.-P. Brantut, and T. Esslinger, Phys. Rev. Lett. **110**, 100601 (2013).
[65] M. Endres, T. Fukuhara, D. Pekker, M. Cheneau, P. Schauß, C. Gross, E. Demler, S. Kuhr, and I. Bloch, Nature (London) **487**, 454 (2012).
[66] M. Schiulaz and M. Müller, AIP Conf. Proc. **1610**, 11 (2014).
[67] W. De Roeck and F. Huveneers, Phys. Rev. B **90**, 165137 (2014).
[68] W. De Roeck, F. Huveneers, M. Müller, and M. Schiulaz, Phys. Rev. B **93**, 014203 (2016).
[69] V. Gurarie and J. T. Chalker, Phys. Rev. B **68**, 134207 (2003).
[70] S. Gopalakrishnan, K. Agarwal, D. A. Huse, E. Demler, and M. Knap, Phys. Rev. B **93**, 134206 (2016).